Autoantigen microarrays for multiplex characterization of autoantibody responses

WILLIAM H. ROBINSON[1,2,4], CARLA DIGENNARO[1,2], WOLFGANG HUEBER[1], BRIAN B. HAAB[5], MAKOTO KAMACHI[1], ERIK J. DEAN[1,2], SYLVIE FOURNEL[6], DEREK FONG[1,2], MARK C. GENOVESE[1], HENRY E. NEUMAN DE VEGVAR[1], KARL SKRINER[7], DAVID L. HIRSCHBERG[2], ROBERT I. MORRIS[8], SYLVIANE MULLER[6], GER J. PRUIJN[9], WALTHER J. VAN VENROOIJ[9], JOSEF S. SMOLEN[7], PATRICK O. BROWN[3], LAWRENCE STEINMAN[2,4] & PAUL J. UTZ[1,4]

[1]*Division of Immunology and Rheumatology, Department of Medicine,* [2]*Department of Neurology and* [3]*Department of Biochemistry and Howard Hughes Medical Institute, Stanford University School of Medicine, Stanford, California, USA*

[4]*Tolerion, Palo Alto, California, USA*

[5]*Van Andel Research Institute, Grand Rapids, Michigan, USA*

[6]*Institut de Biologie Moléculaire et Cellulaire, CNRS, Strasbourg, France*

[7]*Division of Rheumatology, Department of Internal Medicine III, University of Vienna, Vienna, Austria*

[8]*Rheumatology Diagnostics Laboratory, Los Angeles, California, USA*

[9]*Department of Biochemistry, Katholieke Universiteit Nijmegen, Nijmegen, the Netherlands*

Correspondence should be addressed to W.H.R., email: wrobins@stanford.edu

We constructed miniaturized autoantigen arrays to perform large-scale multiplex characterization of autoantibody responses directed against structurally diverse autoantigens, using submicroliter quantities of clinical samples. Autoantigen microarrays were produced by attaching hundreds of proteins, peptides and other biomolecules to the surface of derivatized glass slides using a robotic arrayer. Arrays were incubated with patient serum, and spectrally resolvable fluorescent labels were used to detect autoantibody binding to specific autoantigens on the array. We describe and characterize arrays containing the major autoantigens in eight distinct human autoimmune diseases, including systemic lupus erythematosus and rheumatoid arthritis. This represents the first report of application of such technology to multiple human disease sera, and will enable validated detection of antibodies recognizing autoantigens including proteins, peptides, enzyme complexes, ribonucleoprotein complexes, DNA and post-translationally modified antigens. Autoantigen microarrays represent a powerful tool to study the specificity and pathogenesis of autoantibody responses, and to identify and define relevant autoantigens in human autoimmune diseases.

Autoimmune responses are coordinated by B and T lymphocytes expressing a diverse repertoire of antigen receptors[1], which are not conducive to study with DNA-array technology. In the post-genomics era, the underlying mechanisms and antigen specificity of most autoimmune responses remain poorly understood. A hallmark of autoimmune disease is the production of high-affinity autoantibodies[2]. Although some autoantibodies are involved in cell and tissue damage, neither the pathogenetic role nor the relationship to underlying etiologic events is known for most autoantibodies[2]. Nevertheless, the specificity and pathogenicity of autoantibody responses for certain diseases highlight their potential as important tools for improved diagnosis, classification and prognostication. More importantly, comprehensive profiling of autoantibodies may provide insights into the pathophysiology of autoimmunity, forming the basis for novel treatment strategies such as specific antigen-tolerizing therapy[3–5]. Existing methods to detect autoantibodies are hindered by the many potential autoantigens and requirements for relatively large quantities of each antigen and human sample. To circumvent these limitations, we used miniaturized autoantigen-array technology to perform simple, fluorescence-based, multiplex characterization of human autoantibody responses.

Although conception and initial development of 'multianalyte microspot immunoassays' by Ekins[6] and photolithographically generated peptide arrays by Fodor *et al.*[7] occurred over a decade ago, only recently have several groups reported significant progress developing protein-microarray technologies. Haab *et al.*[8] developed spotted-array-based quantification of 115 antigen–antibody pairs. MacBeath and Schreiber[9] described spotted protein arrays as a tool to detect protein and small-molecule interactions. Methods exist for spotting autoantigens on membranes or derivatized glass slides for detection of autoantibody binding using chemiluminescence-based systems[10]. Others have described ordered array analysis of protein–protein interactions using membranes and filters, polystyrene supports, coated glass slides, nanowell plates and addressable microparticles[11].

The development and validation of simple, large-scale, fluorescence-based autoantigen microarrays for detection of human autoantibodies present in biological fluids such as serum, cerebrospinal fluid and synovial fluid have not yet been described. We refined protein-microarray technology and present generally applicable methods using simple protocols and widely available equipment to study the specificity of autoantibody responses in animals and humans.

Autoantigen arrays

We fabricated 1152-feature arrays containing 196 distinct biomolecules representing major autoantigens targeted by autoantibodies from patients with autoimmune rheumatic diseases. We probed these arrays with mixtures of highly-characterized autoimmune disease serum samples to demonstrate the complexity and diversity of our arrays (Fig. 1). No autoantigen reactivity is demonstrated in a healthy individual (Fig. 1*a*). An array incubated with a mixture of serum derived from three pa-

a

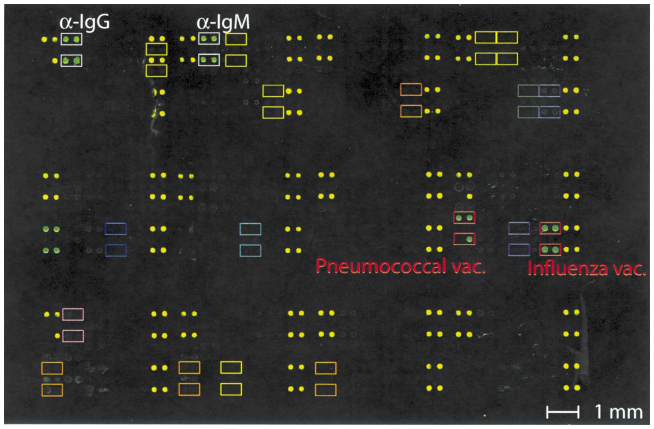

b

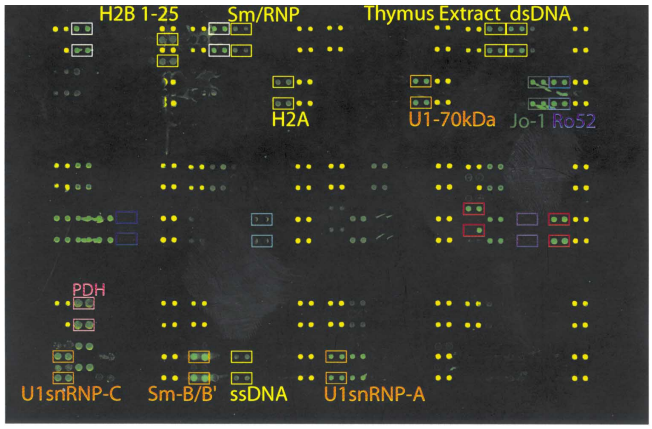

c

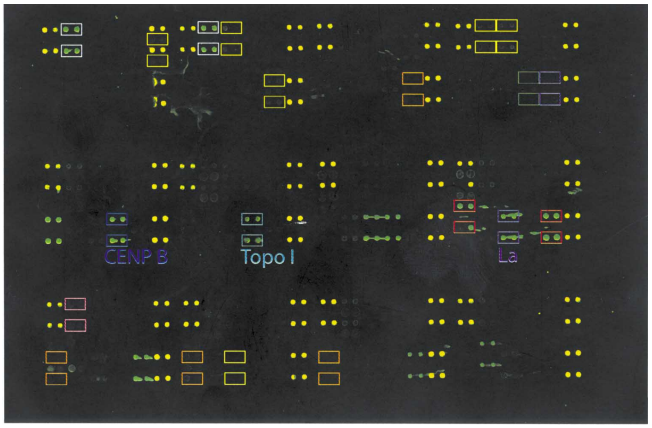

d

Quantitative analysis			
Antigen feature	**Array 1a**	**Array 1b**	**Array 1c**
Histone type II-A	157	2,168	670
Sm/ RNP	275	1,649	505
Double-stranded DNA	167	5,241	448
Single-stranded DNA	6	1,266	166
Histone H2B 1-25	312	1,609	575
Calf Thymus Extract	91	4,111	506
U1snRNP C	344	3,850	294
Sm-B/B'	74	15,157	359
U1snRNP A	135	10,721	112
U1-70kDa	358	6,868	411
Topo I	65	263	3,790
CENP-B	19	19	7,480
PDH	431	2,429	531
Jo-1	41	7,783	63
La	170	0	17,095
Ro52	597	8,426	450
Influenza virus vaccine	26,436	8,319	11,391
Pneumococcal vac.	16,364	5,066	16,365
Anti-human IgM	26,645	24,793	28,586
Anti-human IgG	25,000	25,000	25,000

Fig. 1 The 1152-feature rheumatic disease autoantigen array. Ordered autoantigen arrays were generated by spotting 196 distinct putative autoantigens in 4- or 8-replicate sets using a robotic microarrayer. Spotted antigens include: 36 recombinant or purified proteins including Ro52, La, Jo-1, SR proteins, H2A, Sm-B/B′, U1-70 kD, U1snRNP-C, Sm-B/B′, hnRNP-B1, Sm/RNP complex, topo I, CENP B and PDH; 6 nucleic acid-based putative antigens including several forms of dsDNA and ssDNA; and 154 overlapping and immunodominant peptides representing snRNP proteins, Sm proteins, PARP, and H1, H2A, H3 and H4. We also spotted antibodies specific for human IgG and IgM (α-IgG and α-IgM); the influenza virus and pneumococcal vaccines (vac.); several immunodominant myelin basic protein (MBP) peptides; and a mixture of antibodies pre-labeled with Cy-3- and Cy-5 to serve as 'marker features' to orient the arrays (the yellow features). ***a–c***, Individual arrays were incubated with normal control serum (*a*); a mixture of 3 autoimmune disease sera with known reactivities to dsDNA, ssDNA, histone H2A, SR proteins, Sm/RNP complexes, U1snRNP-C, Sm-B/B′, Ro52, Jo-1 and PDH (*b*); and a mixture of 3 highly-characterized human autoimmune disease sera with known reactivities to La, topo I and CENP B (*c*). Bound antibodies were detected using Cy-3-conjugated goat-anti-human IgM/G before scanning. Most antigen features lacking reactivity contain peptides derived from the histone, snRNP and Sm proteins. Array and autoantigen feature images were false-colored images generated from the scanned digital images of the arrays. Antigen features measured approximately 150 μm in diameter, and can be printed at a density that would allow 15,000 features to be printed in a 1.8 × 5.4-cm area. ***d***, Quantitative analysis of *a–c* with reactive values highlighted.

tients with different diseases—systemic lupus erythematosus (SLE), polymyositis (PM) and primary biliary cirrhosis (PBC)—identified autoantibodies recognizing mammalian double-stranded DNA (dsDNA), synthetic single-stranded DNA (ssDNA), histone H2A, U1-70 kD, U1snRNP-C, SR proteins, Sm-B/B′, Sm/RNP complexes, Ro52, Jo-1 and pyruvate dehydrogenase (PDH) (Fig. 1*b*). A different array incubated with a mixture of serum derived from individual patients with Sjögren syndrome, diffuse scleroderma (sclero-D) or limited scleroderma (sclero-L) demonstrated autoantibodies specifically recognizing centromere protein B (CENP B), topoisomerase I (topo I) and La (Fig. 1*c*). A comparison of the arrays incubated with the mixtures of disease sera confirmed array specificity (Fig. 1*b* and *c*). The results correlate precisely with those obtained for these serum samples using conventional detection methods, including ELISA, immunoprecipitation and western-blot analysis[12].

Array validation and sensitivity analysis

Individual arrays were incubated with mouse monoclonal antibodies specific for human La, Ro52 and Ro60, and a purified

human antibody specific for PDH, followed by the appropriate secondary antibody conjugated to Cy-3 (Fig. 2*b*). Each antibody bound only the antigen feature containing its cognate ligand (Fig. 2*b* and data not shown). Titration of antibodies specific for PDH and La in blocking buffer demonstrates linear detection of antibody concentrations ranging from 1 to 900 ng/ml (Fig. 2*c* and *d*). Direct comparison of antigen arrays with ELISA demonstrated that antigen arrays were consistently 4–8-fold more sensitive for detecting autoantibodies that specifically recognize the five autoantigens tested (Fig. 2*a*).

Autoantigen arrays identify distinct autoantibody profiles

Representative examples of autoantigen array analysis of over 50 highly-characterized autoimmune serum samples are presented (Fig. 3). Shown are published serum samples[12] derived from patients with Sjögren syndrome, SLE, PM, mixed connective-tissue disease (MCTD), PBC, sclero-D, sclero-L and rheumatoid arthritis (RA), identifying distinct and diagnostic autoantibody specificity patterns. For example, we detected SLE-specific autoantibodies directed against DNA and histone (Fig. 3*a*). DNA-specific autoantibodies are pathogenic in some models, and their titers frequently correlate with disease activity[2]. Jo-1 autoantibodies (Fig. 3*a*) frequently predate clinical PM by months to years, and predict development of interstitial lung disease and a poor prognosis[2]. Autoantibodies derived from patients with either sclero-D or sclero-L uniquely target topoisomerase I and CENP B, respectively (Fig. 3*a*). CENP B autoantibodies are associated with a low incidence of interstitial pulmonary and renal disease, whereas the presence of topoisomerase autoantibodies correlates with heightened risk of pulmonary fibrosis and reduced survival[2]. Autoantigen reactivity was not observed when sera from 10 healthy individuals were used as probes, despite reproducible detection of antibodies to pneumococcal and influenza antigens (Fig. 3*a* and data not shown). These array profiles correlated precisely with previously described results of conventional assays[12].

Autoantibody recognition is specific and not crossreactive

We used recombinant his-tagged Ro52, La, U1-70 kD or Jo-1 coupled to agarose beads to deplete specific autoantibody reactivities from diluted serum samples prior to probing arrays (Fig. 4). Using three different serum samples we demonstrated that depletion of serum autoantibodies specific for Ro52 results in a substantial reduction in reactivity at the Ro52 antigen feature, but not at the antigen features containing Jo-1, La or U1-70 kD. Conversely, antibody depletion using beads conjugated with La, Jo-1 or U1-70 kD reduced the reactivity detected at the corresponding antigen features, but not reactivity detected at the

a

	Specificity of human serum									
	α-Jo-1		α-Ro-52		α-La		α-TopoI		α-DNA	
Dilution	Array	ELISA	Array	ELISA	Array	ELISA	Array	ELISA	Array	ELISA
1:40	33,521	141	74,557	137	49,442	188	32,877	141	45,652	717
1:80	26,208	104	52,778	127	45,070	179	29,720	107	38,166	679
1:160	18,214	50	40,687	111	33,865	143	16,678	74	24,655	566
1:320	14,199	14	15,996	81	29,324	91	8,692	38	19,016	333
1:640	4,597	2	15,287	52	16,801	42	5,778	20	14,719	155
1:1,280	1,929	0	8,504	25	6,139	15	1,412	11	4,881	50
1:2,560	650	0	2,534	9	2,322	3	733	2	1,290	12
1:5,120	318	0	1,172	3	967	0	270	0	406	6
1:10,240	217	0	425	0	313	0	102	0	109	1

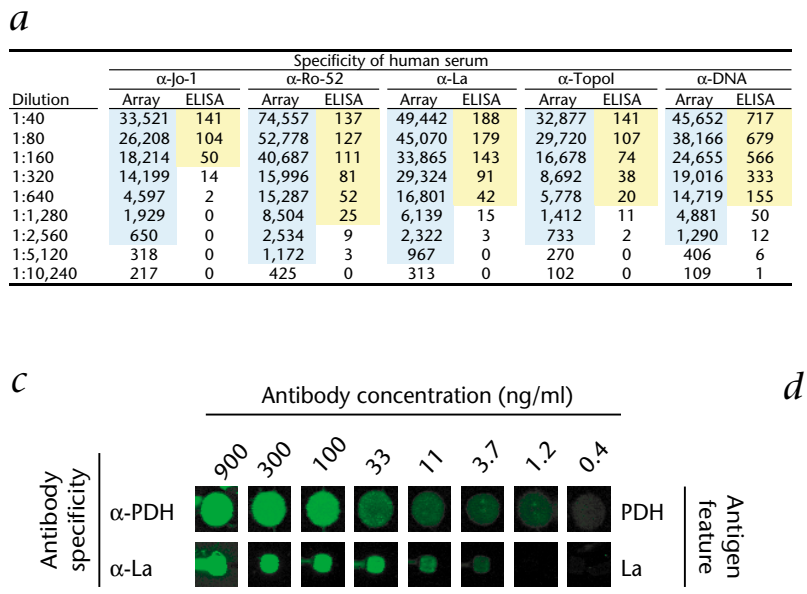

Fig. 2 Array validation and sensitivity analysis. ***a***, Comparison of antigen arrays with ELISA. Human sera containing autoantibodies specific for 5 autoantigens were serially diluted. Identical samples were assayed using antigen arrays and ELISA. Positive reactive values for both array and ELISA analysis are highlighted. Values for anti-DNA reactivity were based on World Health Organization units per ml (negative, 0–93; borderline, 93–139; moderate positive, 139–370; strong positive, >370) and for all other antigens conventional units (negative, <20; moderate positive, 40–80; strong positive, >80). ***b***, Validation of autoantigen arrays using monoclonal and purified human antibodies. Arrays similar to those in Fig. 1 were incubated separately with antibodies against La, Ro52, Ro60 and PDH. Columns of antigen features contained in a single gray box represent features derived from an individual array. ***c***, Titration of antibodies against La and PDH. Images are of representative PDH or La antigen features from individual autoantigen arrays incubated with varying concentrations of purified anti-La or -PDH in blocking buffer. ***d***, Quantitative analysis of the concentration of anti-La or -PDH antibody versus autoantigen feature fluorescence intensity. Shown are mean intensity ± s.d. (represented by the error bars) of the 4 antigen features containing the relevant antigen on each array normalized to the mean intensity of 8 pre-labeled Cy-3-IgG 'marker features'. ■, anti-La; ▲, anti-PDH.

Ro52 antigen feature, demonstrating specific and non-crossreactive autoantibody binding.

Microarray mapping of autoantibody response specificity

The histone H2B 1-25 peptide was identified as a target of the autoantibody response (Fig. 1*b*), and this peptide has been shown to contain a dominant epitope targeted by SLE antibodies[13]. We further characterized this and another serum sample containing autoantibodies recognizing histone peptides derived from distinct histone proteins, each confirmed by parallel ELISA analysis (Fig. 5*a*). These data demonstrate that a subset of linear peptides in a microarray format is bound by serum autoantibodies, enabling epitope mapping of autoantibody responses.

Isotype subclass characterization of autoantibody response

Cy-5-conjugated monoclonal antibodies against three of the human immunoglobulin G (IgG) subclasses bind only the spotted myeloma immunoglobulins of the corresponding subclass (Fig. 5*b*). We used these IgG subclass-specific Cy-5-conjugated antibodies as secondary reagents to determine the IgG subclasses of self-antigen specific autoantibodies (Fig. 5*c*). Arrays incubated with serum derived from a SLE patient followed by Cy-5-conjugated subclass-specific secondary antibodies (and subsequently with Cy-3-conjugated anti-IgG/M antibody) revealed increased binding of autoantibodies of the IgG1 subclass to features of U1-70 kD, and of the IgG3 subclass to features of U1snRNP-C. These features have a yellow hue indicating concomitant binding of the Cy-3-conjugated anti-IgG/M antibody. This demonstrates that autoantigen arrays enable identification of the isotype subclasses of antigen-specific autoantibodies.

Variations in methods for autoantibody detection

We demonstrate use of an alternative comparative fluorescence method for autoantibody detection, enabling comparative quantification using an internal standard[8]. Serum from a control individual and a patient with Sjögren syndrome were directly labeled with either Cy-3 or Cy-5, then analyzed for comparative feature binding on individual arrays. The Ro52- and La-specific autoantibodies in the Sjögren sample were detected as green features in the left panel, which was incubated with Cy-3-labeled Sjögren serum (versus Cy-5-labeled normal serum), and red in the right panel, which was incubated with Cy-5-labeled Sjögren serum (versus Cy-3-labeled normal serum) (Fig. 5*d*).

Discussion

Current techniques to perform large-scale multiplex characterization of autoantibody responses are extremely limited. ELISA, western-blot analysis and radioimmunoassays require relatively large quantities of antigen and patient samples, whereas genetic plaque- and colony-based screening systems are incapable of detecting autoantibodies that recognize post-translational modifications. All such assay systems are not conducive to miniaturization on the micrometer

a

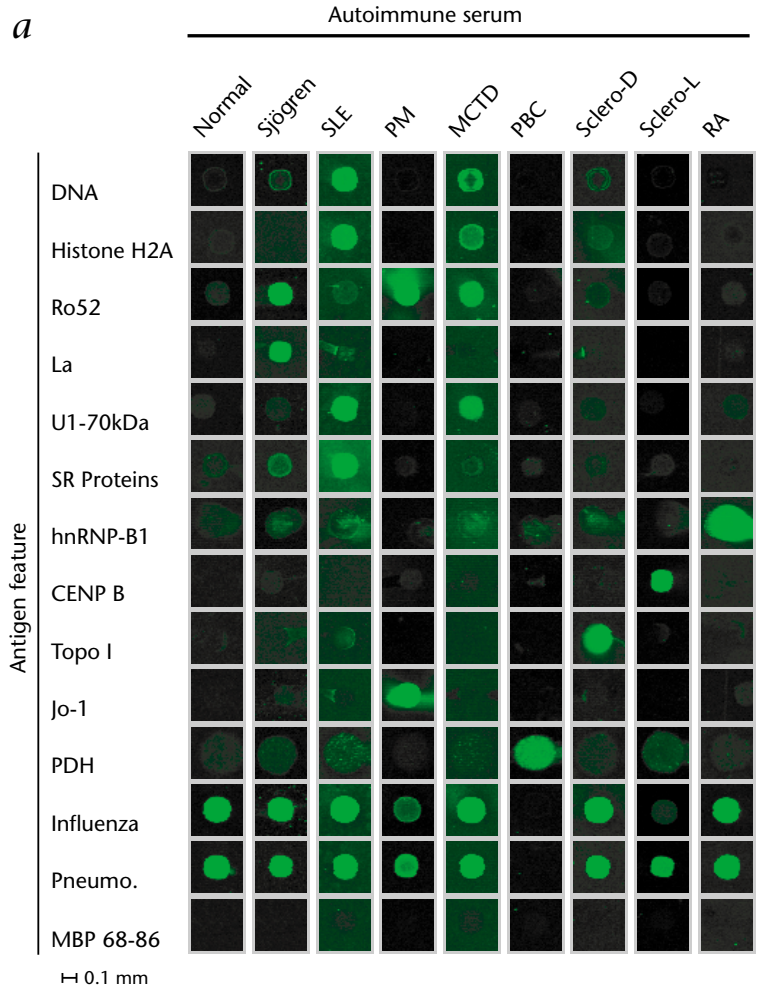

b

Quantitative analysis

Antigen Feature	Normal	Sjögren	SLE	PM	MCTD	PBC	Sclero-D	Sclero-L	RA
DNA	78	352	16,905	0	5,001	1	314	37	26
Histone type II-A	93	44	3,009	0	918	1	100	60	0
Ro52	374	20,934	196	17,396	1,818	93	280	121	143
La	108	8,102	564	0	0	1	119	6	0
U1-70kD	190	135	6,825	31	2,315	159	274	77	153
SR protein	262	629	8,745	112	135	342	237	182	0
hnRNP B1	379	269	1,416	428	978	381	458	317	713
CENP B	12	33	435	21	0	262	11	11,947	0
Topo I	91	113	551	0	11	1	10,095	27	0
Jo-1	24	97	334	28,753	0	1	485	0	3
PDH	190	40	377	40	75	6,609	222	526	279
Influenza virus vac.	15,065	19,809	13,521	1,266	18,686	1	11,641	475	9,134
Pneumococcal vac.	15,580	8,153	29,669	2,779	30,473	1	20,509	5,729	18,374
MBP 68-86	99	13	314	8	0	7	46	40	0

Fig. 3 Identification of disease-specific autoantibodies in human serum. ***a***, Autoantigen arrays were incubated with diluted patient serum samples from a healthy individual for which no specific autoantibody reactivities were detected (normal) or from patients with the indicated diseases. The autoimmune disease serum used to probe each array is indicated along the top of the figure, and each column of antigen features enclosed within a gray box are representative antigen features from a single array. A myelin basic protein peptide recognized on arrays by autoantibodies in serum from rodents with experimental autoimmune encephalomyelitis was included as a representative negative control (MBP 68-86). ***b***, Quantitative analysis.

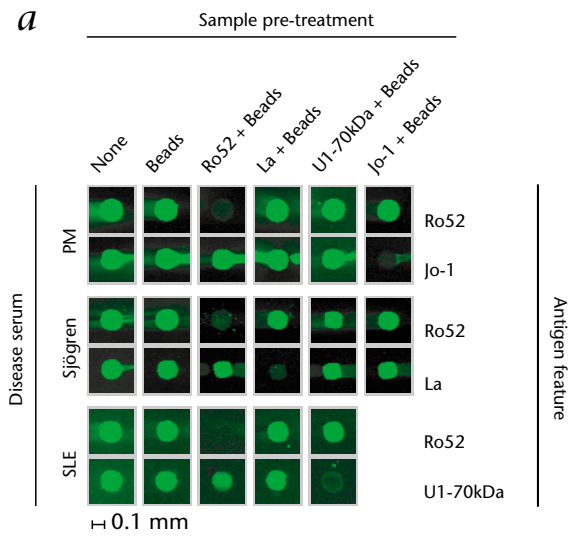

b

Quantitative analysis

Disease Serum	None	Beads	Ro52 + Beads	La + Beads	U1-70kD + Beads	Jo-1 + Beads	Antigen Feature
PM	9,196	2,564	514	2,344	2,748	2,187	Ro52
	10,968	6,674	7,001	6,626	5,195	72	Jo-1
Sjögren	20,934	2,390	72	4,135	5,289	3,296	Ro52
	8,102	988	1,065	23	746	1,090	La
SLE	7,177	2,256	29	2,514	1,772		Ro52
	7,588	2,952	1,774	3,344	202		U1-70kD

Fig. 4 Autoantibody detection is specific. ***a***, Autoantigen arrays were incubated with serum samples from patients with indicated diseases, both without treatment (None), or following 2 rounds of incubation with Ni^{+}-agarose beads alone (Beads) or 2 rounds of depletion of recombinant protein-binding autoantibodies by incubation with indicated proteins, followed by removal of recombinant protein-bound autoantibodies with Ni-agarose beads. Representative antigen features from individual arrays are demarcated by gray boxes. ***b***, Quantitative analysis; reported values represent mean intensities of 4–8 identical antigen features normalized based on the pre-labeled Cy-3/Cy-5 marker spots.

scale or to large-scale autoantibody profiling using limiting quantities of biological fluids. We describe construction and application of ordered autoantigen microarrays to perform simple, low-sample volume, fluorescence-based, multiplex characterization of human autoantibody responses. Our arrays contain hundreds of different putative autoantigens, including proteins, peptides, DNA, enzymatic complexes and ribonucleoprotein complexes. We also detected antibodies specific for phosphorylation-dependent post-translational modifications, which may have an important role in breaking immune tolerance in SLE (data not shown)[14]. Using autoantigen arrays, we demonstrate sensitive and specific detection of

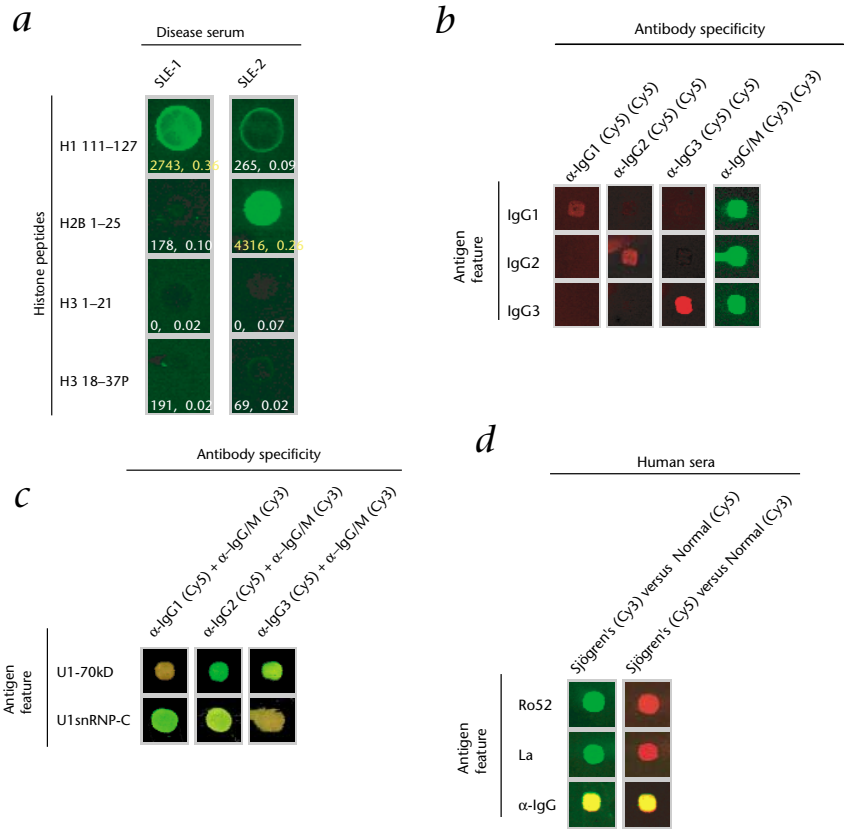

Fig. 5 Antigen arrays for epitope mapping, antibody isotype characterization, and comparative analysis. ***a***, Fine specificity mapping of the anti-histone autoantibody response. Representative antigen features from individual autoantigen arrays incubated with serum from two SLE patients are shown. Numbers on left indicate linear amino-acid sequences of histone peptides. Inset numbers represent normalized median fluorescence intensity of the 4 antigen features containing each peptide, followed by the ELISA result for the corresponding peptide and serum. ELISA results were normalized and interpreted as described[13], and were considered positive when > 0.2. Positive ELISA and array results are indicated in yellow. ***b***, Detection of isotype subclasses. Cy-5-conjugated anti-human IgG subclass-specific antibodies bind spotted IgG of the relevant subclass, but not other subclasses. Purified human myeloma IgG of distinct subclasses was spotted onto arrays. Individual arrays were incubated with the indicated mouse monoclonal anti-human IgG subclass-specific Cy-5-conjugated antibodies or goat-anti-human IgG/M Cy-3-conjugated antisera, and representative antigen features from individual arrays are presented. ***c***, Determination of the IgG isotype subclass of antigen-specific autoantibodies. Arrays were incubated with serum from a SLE patient with known reactivity against U1-70 kD and U1snRNP-C followed by anti-human IgG isotype subclass-specific Cy-5-conjugated monoclonal antibodies and goat-anti-human IgG/M Cy-3-conjugated antisera. The images of the U1-70 kD and U1snRNP-C antigen features for individual arrays incubated with different anti-IgG isotype subclass-specific antibodies are shown. ***d***, Comparative analysis of autoimmune versus control serum directly labeled with distinct spectrally-resolvable fluorochromes. Left, Autoantigen arrays were incubated with an equal mixture of normal control serum directly labeled with Cy-5 (red) and a human Sjögren syndrome serum (with known reactivity to Ro52 and La) directly labeled with Cy-3 (green). Antigens recognized by antibodies in Sjögren syndrome more than normal serum are green, as is observed for Ro52 and La. Equal reactivities are yellow in color (for example, anti-human IgG, bottom row). Right, The converse experiment, in which normal serum is labeled with Cy5 and the Sjögren syndrome sample with Cy3, is shown for comparison.

characteristic autoantibodies in serum derived from patients with eight distinct autoimmune diseases, identification of the isotype of antigen-specific antibodies and detection of antibodies directed against post-translational modifications.

Using fluorescently labeled secondary antibodies, specific autoantibody binding was detected at nanogram per milliliter concentrations, in a linear fashion over a 1000-fold range (Fig. 2*d* and data not shown), and with 4–8-fold greater sensitivity than conventional ELISA (Fig. 2*a*). Due to differences in affinity between antibodies, there is only a relative correlation between signal on the array and the antibody concentration in the sample. For the SLE, Sjögren syndrome, MCTD and sclero-D serum samples presented in Fig. 3, weak reactivity is observed against several additional antigens. This observation is consistent with the frequently broad and overlapping autoantibody response patterns observed in these rheumatic diseases[2], combined with the increased sensitivity of antigen arrays.

For practical reasons we have focused on using secondary antibodies, including isotype-specific antibodies, covalently conjugated to spectrally resolvable fluorochromes. This eliminates the need for direct labeling of individual patient samples, which is expensive, labor intensive and subject to sample-to-sample variability in labeling efficiency (data not shown). Autoantigen-array technology is not without limitations. A number of spotted autoantigens (for example, certain Sm and histone proteins) were not detectable in this format, presumably due to loss of three-dimensional structures, steric interferences or electrostatic repulsion. An important direction for refinement of this method is improvement of surfaces and conditions for attachment of structurally and chemically heterogeneous autoantigens.

Identification of autoantigen targets of B and T lymphocytes has a central role in understanding the pathogenic mechanisms governing the initiation and propagation of autoimmune diseases. The utility of autoantibody profiling is based in part on the hypothesis that the overall specificity of the autoantibody re-

Methods

Peptides, proteins, antibodies and sera. Reagents were obtained from the following sources: peptides derived from Sm-D, hnRNP-A2, the 70-kD component of the U1 small nuclear ribonucleoprotein complex (U1-70 kD), poly A ribose polymerase (PARP) and histones H1, H2A, H2B, H3 and H4 (synthesized in the laboratory of S.M.); recombinant his-tagged Ro52, La, histidyl-tRNA synthetase (Jo-1), Sm-B/B′, the C component of the U1 small nuclear ribonucleoprotein complex (U1snRNP-C), U1-70 kD, topoisomerase I, CENP B, thyroglobulin and thyroid peroxidase (KMI Diagnostics, Minneapolis, Minnesota) and hnRNP-B1 (ref. 19); purified vimentin, pyruvate hydrogenase complex (PDH), transglutaminase, DNA, histone H2A, RNA polymerase, cardiolipin, rRNA and human myeloma immunoglobulins (Sigma); Sm/RNP complex (ImmunoVision, Springdale, Arizona); monoclonal mouse antibodies against La, Ro52, and Ro60 (ref. 20); Cy-3-conjugated goat-anti-human IgG/M antisera (Jackson Immunoresearch, West Grove, Pennsylvania); influenza virus (FluShield) and pneumococcal (Pneumovax) vaccines; and anti-human IgG subclass-specific monoclonal antibodies (Southern Biotechnology Associates, Birmingham, Alabama). Patients' sera were described[12] or were Arthritis Foundation/CDC Reference Sera (Centers for Disease Control, Atlanta, Georgia).

Conjugation of antibodies and human serum to spectrally resolvable fluorochromes. NHS-ester-activated Cy-3 and Cy-5 dye packs (Amersham) were resuspended in 0.1 M sodium carbonate buffer (pH 8.5), mixed with purified antibody or human serum, and quenched with 10% volume 1 M Tris according to the manufacturer's instructions. Free dye was removed by three PBS wash-spin cycles in Microcon centrifugal filter units with 100,000 nominal molecular weight limits (Millipore, Bedford, Massachusetts).

Autoantigen array fabrication. Antigens were diluted in PBS or water to 0.2 mg/ml solutions, and transferred into 384-well plates. A robotic microarrayer using ChipMaker 2 Micro Spotting Pins (TeleChem International, Sunnyvale, California) was used to spot the antigens and antibodies onto poly-L lysine-coated microscope slides (CEL Associates, Pearland, Texas) in an ordered array as described[8,9] (see http://brownlab.stanford.edu/). The spotted microarrays were stored at 4 °C and maintained reactivity for months. The 1152-feature autoantigen arrays were used for all experiments described in Figs. 1–5.

Pretreatment of samples. In Fig. 4, diluted serum samples were incubated with Ni^{+}-nitrilotriacetic acid (NTA)-agarose beads alone (Qiagen, Valencia, California), or 2 rounds of 1-h incubations with 10 μg of his-tagged recombinant Ro52, La, Jo-1 or U1-70 kD (KMI Diagnostics) followed by addition of Ni^{+}-NTA-beads, incubation, and removal by centrifugation.

Probing and scanning autoantigen arrays. Arrays were circumscribed with a hydrophobic marker PAP pen followed by overnight blocking at 4 °C in PBS with 0.5% Tween-20 and 3% FCS (3% non-fat milk was also an effective blocking agent) in a metal-slide rack in a glass histology dish. Arrays were incubated in histology chambers for 1.5 h at 4 °C with 300 μl (or 30 μl under a glass cover slip when patient samples were limiting) of 1:150 dilutions of the relevant serum in blocking buffer. Arrays were rinsed and washed twice for 15 min rotating in blocking buffer. Arrays were then incubated with 300 μl of a 1:3000 dilution of goat-anti-human Cy3-conjugated secondary antibody for 1 h at 4 °C, rinsed, and washed twice for 30 min in blocking buffer, twice for 20 min in PBS and twice for 15-second washes in water. Arrays were spun dry and scanned using a GenePix 4000 Scanner, and GenePix Pro 3.0 software was used to determine median intensities of feature and background pixels (Axon Laboratories, Foster City, California). For all figures, unless noted otherwise, intensity levels represent median values from 4–8 identical antigen features (using the (median feature pixel intensity – median background pixel intensity) for each individual feature) on each array normalized to median anti-IgG feature intensity from 8 features. Threshold values for determining reactivity were set at 4-fold above the background intensity calculated based on the aggregate mean intensity of 4 different negative control antigen features (8 replicates per array of each) for all arrays in the study.

ELISA. ELISA results presented in Fig. 2*a* were performed using optimized commercial assays by a clinical laboratory (Rheumatology Diagnostics Laboratory, Los Angeles, California) and in Fig. 5*a* as decribed[13].

sponse correlates with helper T-cell autoreactivity, which drives many autoimmune diseases[15]. For many human autoimmune diseases, autoreactive B- and T-cell responses are directed against the same targeted autoantigens, and in some cases the same immunodominant epitopes[16–18]. Even if there is discordance between the fine specificity of the B- and T-cell responses, the ability to use autoantigen arrays to identify the specific self-protein(s) targeted by the autoimmune response is of tremendous value for identifying and evaluating candidate autoantigens.

Autoantigen arrays provide a practical means to analyze biological fluids for autoantibodies directed against thousands of distinct autoantigens in a low-cost and low-sample volume format. There is a variety of potential applications of autoantigen-array technology, for example: 1) rapid screening for autoantibody specificities associated with autoimmune diseases to facilitate early diagnosis and treatment; 2) characterization of the specificity, diversity and epitope spreading of autoantibody responses; 3) determination of isotype subclass of antigen-specific autoantibodies to assess their potential pathogenicity (for example, complement-fixing versus non-fixing IgG subclasses) and the relative Th1 versus Th2 bias of the autoimmune response against a particular antigen[15]; 4) guiding development and selection of antigen-specific therapies for use in the clinic[3–5]; and 5) as a discovery tool to identify novel autoantigens or epitopes. Using analogous methodology, antigen-array technology could be applied to study immune responses to, and elicited by vaccines against, viruses, bacteria and tumors. The adaptations of methods and protocols described in this report, and in greater detail at http://www.stanford.edu/group/antigenarrays/ and http://brownlab.stanford.edu/, provide simple and easily adoptable methods to perform autoantibody profiling using widely-available spotted DNA-array equipment.

Acknowledgments

We thank K. Chong and D. Mitchell for their outstanding assistance; J.G. Lindsay for antibodies; and A. Abeliovich, H. Garren, P. Ruiz and G. Hermans for insightful discussions. This work was primarily supported by a Howard Hughes Postdoctoral Research Fellowship for Physicians Award, NIH K08 AR02133 and Arthritis Foundation Chapter Grant to W.H.R; NIH/NINDS 5R01NS18235 and NIH U19DK61934 to L.S.; and NIH K08 AI01521, an Arthritis Foundation Investigator Award, a Baxter Foundation Career Development Award, a Stanford University Office of Technology Licensing Award, and NIH U19 DK61934 to P.J.U. P.O.B is an Associate Investigator of the Howard Hughes Medical Institute.

1. Steinman, L. A few autoreactive cells in an autoimmune infiltrate control a vast population of nonspecific cells: A tale of smart bombs and the infantry. *Proc. Natl. Acad. Sci. USA* **93**, 2253–2256 (1996).
2. von Mühlen, C.A. & Tan, E.M. Autoantibodies in the diagnosis of systemic rheumatic diseases. *Semin. Arthritis. Rheum.* **24**, 323–358 (1995).
3. Brocke, S. *et al.* Treatment of experimental encephalomyelitis with a peptide analogue of myelin basic protein. *Nature* **379**, 343–346 (1996).
4. Critchfield, J.M. *et al.* T cell deletion in high antigen dose therapy of autoimmune encephalomyelitis. *Science* **263**, 1139–1143 (1994).
5. Garren, H. *et al.* Combination of gene delivery and DNA vaccination to protect from and reverse Th1 autoimmune disease via deviation to the Th2 pathway. *Immunity* **15**, 15–22 (2001).
6. Ekins, R.P. Multi-analyte immunoassay. *J. Pharm. Biomed. Anal.* **7**, 155–168 (1989).
7. Fodor, S.P. *et al.* Light-directed, spatially addressable parallel chemical synthesis. *Science* **251**, 767–773 (1991).
8. Haab, B.B., Dunham, M.J. & Brown, P.O. Protein microarrays for highly parallel detection and quantitation of specific proteins and antibodies in complex solutions. *Genome Biol.* **2**, research0004.1-0004.13 (2001).
9. MacBeath, G. & Schreiber, S.L. Printing proteins as microarrays for high-throughput function determination. *Science* **289**, 1760–1763 (2000).
10. Joos, T.O. *et al.* A microarray enzyme-linked immunosorbent assay for autoimmune diagnostics. *Electrophoresis* **21**, 2641–2650 (2000).
11. Robinson, W.H., Steinman, L. & Utz, P.J. Proteomics technologies in the study of autoimmune disease. *Arthritis. Rheum.* **46**, 886–894 (2002).
12. Utz, P.J., Hottelet, M., Schur, P.H. & Anderson, P. Proteins phosphorylated during stress-induced apoptosis are common targets for autoantibody production in patients with systemic lupus erythematosus. *J. Exp. Med.* **185**, 843–854 (1997).
13. Monestier, M., Decker, P., Briand, J.P., Gabriel, J.L. & Muller, S. Molecular and structural properties of three autoimmune IgG monoclonal antibodies to histone H2B. *J. Biol. Chem.* **275**, 13558–13563 (2000).
14. Utz, P.J., Gensler, T.J. & Anderson, P. Death, autoantigen modifications, and tolerance. *Arthritis Res.* **2**, 101–114 (2000).
15. Abbas, A.K., Murphy, K.M. & Sher, A. Functional diversity of helper T lymphocytes. *Nature* **383**, 787–793 (1996).
16. Lu, L., Kaliyaperumal, A., Boumpas, D.T. & Datta, S.K. Major peptide autoepitopes for nucleosome-specific T cells of human lupus. *J. Clin. Invest.* **104**, 345–355 (1999).
17. Yeaman, S.J., Kirby, J.A. & Jones, D.E. Autoreactive responses to pyruvate dehydrogenase complex in the pathogenesis of primary biliary cirrhosis. *Immunol. Rev.* **174**, 238–249 (2000).
18. Warren, K.G., Catz, I. & Steinman, L. Fine specificity of the antibody response to myelin basic protein in the central nervous system in multiple sclerosis: the minimal B-cell epitope and a model of its features. *Proc. Natl. Acad. Sci. USA* **92**, 11061–11065 (1995).
19. Steiner, G. *et al.* Purification and partial sequencing of the nuclear autoantigen RA33 shows that it is indistinguishable from the A2 protein of the heterogeneous nuclear ribonucleoprotein complex. *J. Clin. Invest.* **90**, 1061–1066 (1992).
20. Pruijn, G.J., Simons, F.H. & van Venrooij, W.J. Intracellular localization and nucleocytoplasmic transport of Ro RNP components. *Eur. J. Cell. Biol.* **74**, 123–132 (1997).

ON THE MARKET

CELL PICKING/TRANSFER

Automated cell selection and transfer.

The Quixell **cell selection and transfer system** from Stoelting uses automated micromanipulation to pick up and transfer single cells — one cell at a time — and deposit them into isolated growth chambers. The desired cell is targeted with a joystick movement, and with a few keystrokes, collected into a micropipette. Another single keystroke automatically transfers and deposits the cell in the next sequential well on a microtiter. Stoelting says Quixell allows the operator to place exactly one cell in each well. The system includes a motorized microscope stage capable of holding 'source' and 'destination' plates, a *z*-axis drive to position the pipette system precisely, and an electronic unit for microprocessor-controlled selection and transfer.

Tel. (+1) 630-860-9700
www.stoeltingco.com

HANDY HELPERS

Vacuum protection system for supernatant aspiration.

C.B.S. Scientific offers a line of **vacuum protection systems** for use in the aspiration of standard, radioactive and pathogenic supernatants. Housed in either a clear acrylic cabinet for protection against